

How is spatial homogeneity in precipitation extremes changing globally?

Ankit Ghanghas¹, Ashish Sharma², Sayan Dey¹, and Venkatesh Mohan Merwade¹

¹Purdue University

²University of New South Wales

January 20, 2023

Abstract

The effect of climate change on precipitation intensity is well documented. However, findings regarding changes in spatial extent of extreme precipitation events are still ambiguous as previous studies focused on particular regions and time domains. This study addresses this ambiguity by investigating the pattern of changes in the spatial extent of short duration extreme precipitation events globally. A grid-based indicator termed Spatial-Homogeneity (SH) is proposed and used to assess the changes of spatial extent in Global Precipitation Measurement (GPM) records. This study shows that i) rising temperature causes significant shrinking of precipitation extent in tropics, but an expansion of precipitation extent in arid regions, ii) storms with higher precipitation intensity show a faster decrease in spatial extent, iii) larger spatial extent storms are associated with higher total precipitable water. Results imply that in a warming climate, tropics may experience severe floods as storms may become more intense and spatially concentrated.

Hosted file

supplementary_information_paper.docx available at <https://authorea.com/users/578332/articles/620340-how-is-spatial-homogeneity-in-precipitation-extremes-changing-globally>

1
2 **How is spatial homogeneity in precipitation extremes changing globally?**
3

4 **Ankit Ghanghas¹, Ashish Sharma², Sayan Dey¹ and Venkatesh Merwade¹**
5

6 ¹ Lyles School of Civil Engineering, Purdue University, West Lafayette, IN, USA

7 ² School of Civil and Environmental Engineering, University of New South Wales, Sydney, New
8 South Wales, Australia.

9
10
11 Corresponding author: Ankit Ghanghas (aghangha@purdue.edu)
12

13 **Key Points:**

- 14 • A global trend of moisture accumulation towards the storm center as spatial extent
15 decreases with a rise in temperatures
- 16 • Rising temperature causes significant shrinking of precipitation extent in tropics, but an
17 expansion in arid regions and central Europe.
- 18 • Storms with higher precipitation intensity show a faster decrease in spatial extent.
19

20 Abstract.

21 The effect of climate change on precipitation intensity is well documented. However, findings
22 regarding changes in spatial extent of extreme precipitation events are still ambiguous as
23 previous studies focused on particular regions and time domains. This study addresses this
24 ambiguity by investigating the pattern of changes in the spatial extent of short duration extreme
25 precipitation events globally. A grid-based indicator termed Spatial-Homogeneity (SH) is
26 proposed and used to assess the changes of spatial extent in Global Precipitation Measurement
27 (GPM) records. This study shows that i) rising temperature causes significant shrinking of
28 precipitation extent in tropics, but an expansion of precipitation extent in arid regions, ii) storms
29 with higher precipitation intensity show a faster decrease in spatial extent, iii) larger spatial
30 extent storms are associated with higher total precipitable water. Results imply that in a warming
31 climate, tropics may experience severe floods as storms may become more intense and spatially
32 concentrated.

33

34 Plain Language Summary.

35 Variation in extreme precipitation patterns can significantly impact flood risk, ecology as well as
36 the efficacy of water supply and management strategies. With a changing climate, there is an
37 overarching need to understand how alterations in climate changes precipitation patterns,
38 particularly those corresponding to extreme precipitation events. Analyzing the intensity (amount
39 of rainfall/hour) of precipitation, spatial extent of the precipitation event, duration of the
40 precipitation event and total volume of precipitated water are key to understanding these extreme
41 precipitation events. There is a clear consensus among the scientific community that higher
42 temperatures result in more intense precipitation events, but the effect of temperature on spatial
43 extent is still debated. This study uses a new Spatial-Homogeneity metric to analyse the global
44 changes in spatial extent of extreme precipitation storms. The study finds that a higher
45 temperature results in smaller size extreme storms in the tropics, but larger size storms in the arid
46 regions. It is also observed that more intense precipitation events have smaller spatial extent,
47 implying that rising temperatures will result in spatially smaller and more intense extreme
48 precipitation storms.

49

50 **1 Introduction**

51 The devastation from flash floods particularly in rapidly urbanizing environments is well
52 documented, as intense precipitation storms can quickly turn into walls of water in highly
53 impervious areas (Hapuarachchi et al., 2011). One of the greatest challenges to understanding
54 flash floods is to understand the spatial and temporal distribution of precipitation, particularly of
55 intense short period precipitation bursts (Archer & Fowler, 2018; Kelsch Matthew and Caporali,
56 2001). Knowledge of how such patterns change with time or with the intensity of the
57 precipitation experienced, is of considerable use in designing effective stormwater systems and
58 preparing for changes in climate.

59

60 The variation of extreme-precipitation intensity with temperature is well documented,
61 underpinning the understanding of how extreme precipitation patterns might change in future
62 (Hardwick Jones et al., 2010; Lenderink et al., 2011; Lenderink & van Meijgaard, 2008; Mishra
63 et al., 2012; Utsumi et al., 2011; Westra et al., 2014). It is generally accepted that in a warming
64 climate the intensity of an extreme precipitation will increase because precipitation depends on
65 the atmospheric water content which increases exponentially with temperature, as governed by
66 the Clausius-Clapeyron(C-C) relationship (Roderick et al., 2019, 2020; Trenberth et al., 2003;
67 Visser et al., 2021). While global daily precipitation exhibits a sensitivity (or scaling) of around
68 6-7%/°C (C-C rate) with rise in temperature (Kharin et al., 2013; Pall et al., 2007; Tebaldi et al.,
69 2006), short duration (sub-daily and sub-hourly) precipitation storms are observed to scale at
70 rates ranging from C-C to 2 C-C (called super C-C scaling) (Berg et al., 2013; Hardwick Jones et
71 al., 2010; Lenderink et al., 2017; Lenderink & van Meijgaard, 2008; Mishra et al., 2012; Westra
72 et al., 2014). This super C-C scaling is hypothesized to be a result of change in storm dynamics,
73 particularly the morphing of the storm extent and underlying structure (Collins et al., 2013;
74 Lenderink & van Meijgaard, 2008).

75

76 Unlike the general acceptance of variation in intensity, the variation in the spatial extent of short
77 duration storms is still debated with two contrasting hypotheses. The first hypothesis suggests a
78 decreasing spatial extent with rising temperature due to dynamic factors dominating the storm
79 dynamics, thereby redistributing the moisture towards the center (Figure 1a) (Wasko et al.,

80 2016). The second, contrasting, hypothesis, suggests that if the thermodynamic factors dominate,
81 rising temperature would result in increasing spatial extent owing to stronger cloud dynamics
82 and larger shower clusters which will bring more moisture from larger areas (Lochbihler et al.,
83 2017). Findings from numerous studies analyzing the effect of temperature on spatial extent
84 support the decreasing spatial extent hypothesis (Chang et al., 2016; Guinard et al., 2015; Han et
85 al., 2020; J. Li et al., 2018; Peleg et al., 2018; Wasko et al., 2016), and several other support the
86 increasing spatial extent hypothesis (Bevacqua et al., 2021; Chen et al., 2021; Lochbihler et al.,
87 2017; Matte et al., 2022), while some others present no effect of temperature on spatial extent
88 (Manola et al., 2018). However, most past studies have focused on specific regions, or on certain
89 types of storms, or at daily precipitation extremes rather than short duration storms.

90

91 To address the ambiguity of whether short duration precipitation extents are expanding or
92 shrinking with rising temperature, this study investigates the global patterns of change in spatial
93 extent. This study proposes a novel metric to quantify grid-homogeneity termed Spatial-
94 Homogeneity (SH) to compare the changes in spatial extent of extreme storms with different
95 intensity and at different locations. The spatial-homogeneity metric can be used for radar as well
96 as satellite measurements and is applicable for both short and long duration precipitation
97 extremes. The study first investigates the global variability in spatial extent of short duration
98 extreme storms in the recent past. Subsequently the relationship between temperature and spatial
99 extent is examined. Finally, the study explores how total precipitable water, warm versus cold
100 years and wet versus dry years impact the spatial extent.

101

102 Even though the satellite products are known to underestimate rainfall rates for deep convective
103 systems (Adhikari et al., 2019; Dinku et al., 2010; Duan et al., 2015; Kucera & Klepp, 2022; R.
104 Li et al., 2021), their high spatio-temporal resolution and global coverage make them useful in
105 assessing change in the spatial extent of precipitation. Therefore, to have an acceptable global
106 resolution, this study adopts satellite data products instead of the sparsely gauged ground
107 observations available to represent variability in spatial extent across the world and to infer
108 changes in this variability with local climatic variables including temperature, precipitation
109 intensity and total precipitable water.

110

111 **2 Data and Methods**

112 The Integrated Multi-satellite Retrievals for Global Precipitation Measurement (IMERG)
113 (version 6) dataset provides continuous records of satellite precipitation observation from 2000 -
114 present, as the IMERG algorithm combines the early precipitation estimates from Tropical
115 Rainfall Monitoring Mission (TRMM) (2000-2015) with the more recent precipitation estimates
116 from Global Precipitation Measurement (GPM) (2014-present) (Huffman et al., 2020). However,
117 to maintain the homogeneity of records only GPM IMERG estimates from 2014 to 2022 are used
118 in this study. Due to the focus of this study on spatial extent of instantaneous/extreme
119 precipitation bursts, analysis is performed on IMERG's high spatial and temporal resolution
120 3IMERGHH (version 6) (Huffman et al., 2020) product available at $0.1^\circ \times 0.1^\circ$ spatial
121 resolution and 30 minute time step. Earth ReAnalysis (ERA5), produced by European Center for
122 Medium-Range Weather Forecasts (ECMWF), provides global reanalysis data for both
123 temperature and moisture (Hersbach et al., 2020). ERA5 combines historical observations with
124 the Integrated Forecasting System (IFS) Cy41r2 model to produce hourly outputs of numerous
125 atmospheric, land and oceanic climate variables. Hourly Integrated Water Vapor (IWV) or Total
126 Column Water Vapor (TCWV) at $0.25^\circ \times 0.25^\circ$ spatial resolution is used in this study. Hourly
127 2m surface air temperature at $0.1^\circ \times 0.1^\circ$ spatial resolution are obtained from the land
128 component of ERA5, the ERA5-Land dataset (Muñoz-Sabater et al., 2021).

129

130 To analyze the spatial extent of extreme precipitation events, independent storm fields must be
131 identified. In this study, a storm field is defined by considering a grid cell with extreme
132 precipitation and its eight neighboring cells such that the center pixel corresponds to the center of
133 the storm and receives more precipitation than the neighboring cells. To identify independent
134 storm fields, the top ten Annual Maximum Precipitation (AMP) events at each grid cell of the
135 GPM dataset are estimated for each year in the dataset. Further, for each grid cell, the
136 precipitation for the eight neighboring cells surrounding the central precipitation event is
137 extracted for the same time of occurrence as the central extreme precipitation event and
138 compared to the center cell. If, for instance, the AMP event at the center cell has the same or
139 lower precipitation than one of its eight neighbors, then the next maximum event (out of the top

140 ten annual maximum events) is considered and compared with neighboring precipitation at the
 141 time of its occurrence. The validity of independent storm field is enforced by choosing only the
 142 maximum event out of the top ten maximum events which has greatest intensity at the center cell
 143 than its neighbors.

144

145 A new metric, “Spatial Homogeneity” denoted SH, is proposed to investigate and compare the
 146 changes in spatial extent of varying intensity extreme storms and at different locations. To
 147 understand the homogeneity metric for an extreme storm, precipitation for all the cells in the
 148 storm field is sorted in descending order of its intensity and a cumulative normalization
 149 performed. Consider the precipitation in descending order is represented as $P_0, P_1, P_2, P_3, P_4, P_5,$
 150 P_6, P_7, P_8 where in P_0 is maximum precipitation and lies at the center of the storm field. The
 151 study ascertains the spatially accumulated precipitation average as $P_0/1, (P_0+P_1)/2,$
 152 $(P_0+P_1+P_2)/3, \dots, (P_0+P_1+P_2+P_3+P_4+P_5+P_6+P_7+P_8)/9$. Here the last term represents
 153 average precipitation for the entire grid for the extreme storm event considered. These values are
 154 then plotted against the number of grid points considered in formulating the accumulated spatial
 155 average. The above accumulated precipitation distribution can be compared to the case where all
 156 neighbors have zero precipitation and only the center point received precipitation. In this
 157 scenario, the accumulated rainfall plot would represent $P_0/1, (P_0)/2, (P_0)/3 \dots \dots (P_0)/9$ against
 158 the number of grid points associated. The other comparison represented the case where all grid
 159 points receive the same amount of precipitation say P_0 , resulting in a constant value (P_0) being
 160 depicted against the number of grid cells. An assessment of the spatial distribution of each storm
 161 is then formulated by noting how strongly the actual extreme event deviated from the two
 162 extreme cases considered. This assessment is depicted in Figure 1b giving an overview of the
 163 methodology adopted in assessing the spatial structure of the extreme precipitation event
 164 surrounding the central grid cell. The Spatial Homogeneity metric SH calculated using Equation
 165 1 is used to ascertain the spatial homogeneity or inhomogeneity of the extreme storm field.

$$SH = \frac{a}{a+b} = \frac{\frac{1}{9} \times \sum_{i=0}^8 P_i - \frac{P_0}{9}}{P_0 - \frac{P_0}{9}} \quad (1)$$

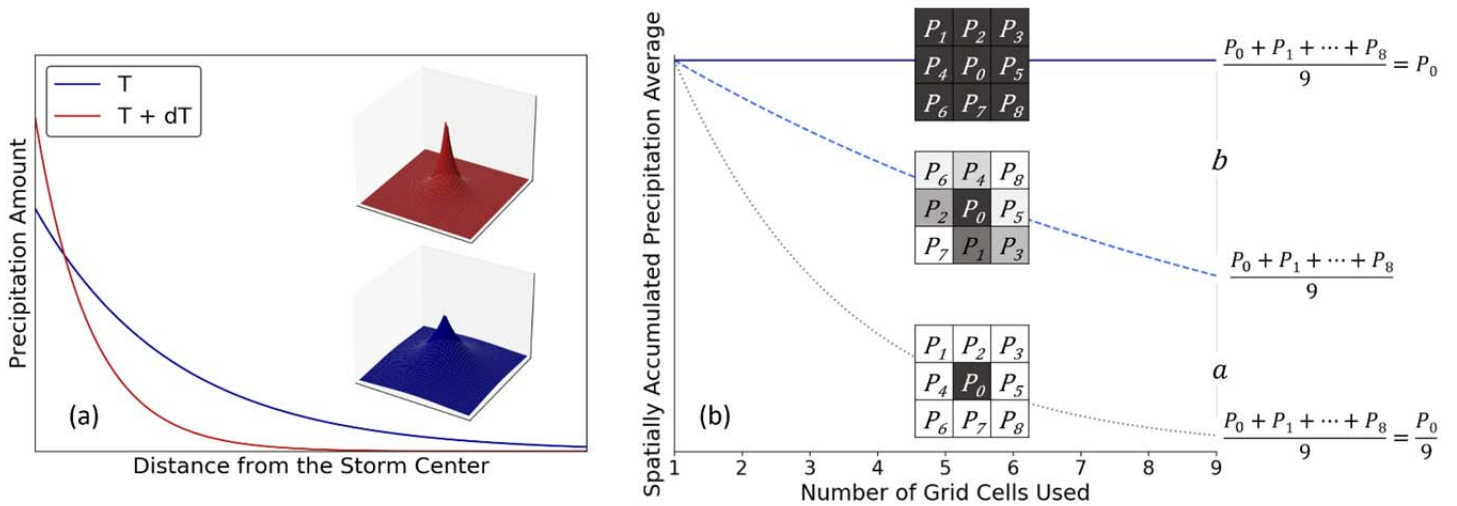


Figure 1. a) Depiction of increasing convection hypothesis, an increase in temperature results in higher intensity and redistribution of moisture towards storm center. Blue indicates lower temperature and red indicates higher temperature. Three-dimensional curves are also presented to emphasize the hypothesis. b) Representation of the SH methodology. Nine boxes represent the eight neighbors around the highest intensity center. The intensity of grey in each box indicates the intensity of rainfall at that grid.

166

167 The Spatial Homogeneity metric allows a comparison of the extreme storm from a fully uniform
 168 case to a case where an isolated extreme falls at the center of the grid. If a warmer future creates
 169 more isolated and convective rainfall events, the above metric will collapse to zero. If the
 170 opposite were to occur (more uniform rainfall extremes) the metric will assume a value of one.
 171 The increasing convection hypothesis outlined above is depicted in Figure 1a. The SH metric
 172 allows assessment of spatial distribution of extreme precipitation events without focusing on the
 173 intensity of the event as well as assessment of the spatial distribution of extreme events across
 174 the world.

175 A sensitivity assessment of SH with associated temperature is performed using quantile
 176 regression with a focus on the median (50th percentile). The resulting regression coefficient is
 177 referred to as “sensitivity” in the remainder of this paper. The quantile regression sensitivity
 178 estimator by Wasko & Sharma (2014) has been adopted in this study. As only annual maximum
 179 precipitation (AMP) events are considered, the assessment results presented focus on the 50th
 180 percentile (median) instead of rarer percentiles. Details of the sensitivity estimation procedure,

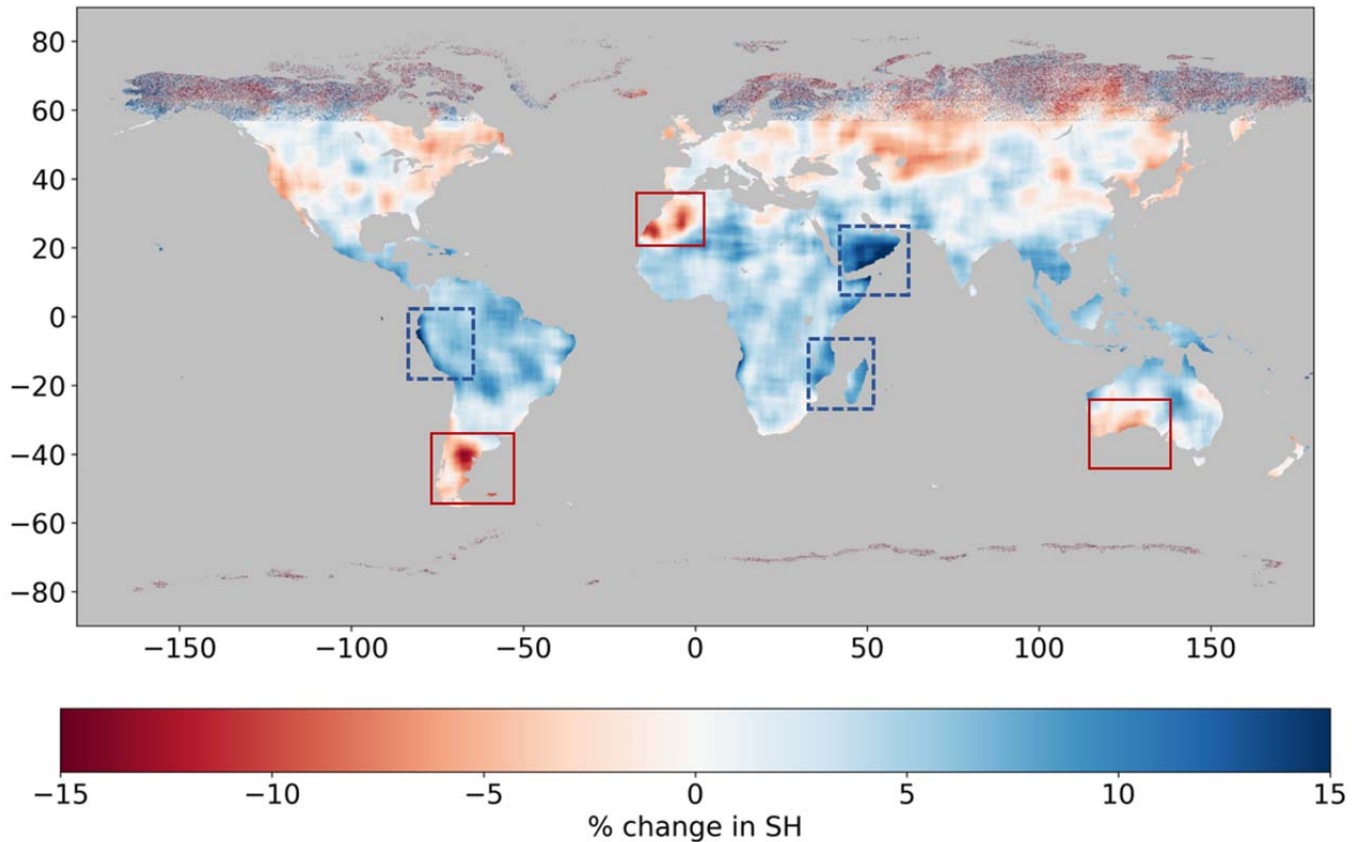
181 its sensitivity to computational needs, and its motivation in the context of identifying trends in a
182 highly variable response, are presented in Wasiko & Sharma (2014) and Sharma et al. (2018).

183 **3 Results**

184 **3.1.Changes in of Spatial Homogeneity (Spatial Extent) in recent past**

185 The Spatial-Homogeneity metric does not give a quantitative estimate of the exact spatial extent
186 of the storm, but it is a quick and resourceful method to track the changes in spatial extent of
187 storm. The SH-metric can also be used to understand the geographic distribution of spatial extent
188 across the globe. The average SH-metric for AMP 30-min storms (Figure S1 in supporting
189 information) shows smaller storm extents in tropics and mountainous regions. This is coherent
190 with the findings of Tan et al. (2021), which concluded that extreme storms in tropics are
191 typically smaller than those in northern and southern temperate regions.

192
193 Figure 2 presents the average change in SH between 2014 to 2021 with reference to the 2014 SH.
194 A running median of $4^{\circ} \times 4^{\circ}$ grid has been used to smooth out the variability. The changes in SH
195 from year to year are presented in Figure S2 in supporting information. The spatial extent of
196 storms in the equatorial regions between 20° N and 20° S has increased homogeneously over the
197 years. The equator observes a significant and spatially consistent increase in spatial extent of
198 storms. On the other hand, regions north of 30° N and south of 30° S have experienced spatially
199 smaller storms in the recent years. The change of storm extent in these regions are inconsistent
200 and sporadic increase in storm size can also be observed. Storms in the Arabian Peninsula, some
201 parts of Africa near Mozambique and Madagascar, Mexico and parts of South America near Peru
202 and Bolivia have consistently and significantly increased over the recent years. Contrasting
203 results are observed in Northwest Africa around Morocco and Western Sahara, southern
204 Argentina (Patagonian Dessert), and southern Australia, where storm sizes have consistently and
205 significantly decreased in the immediate past.



206

207 *Figure 2. A $4^{\circ}\times 4^{\circ}$ median of Average Change in SH between 2014 to 2021 with reference to*
 208 *2014 SH. Decrease in SH (spatial extent) is shown in red and increase in SH (spatial extent) is*
 209 *shown in blue. Boxes highlight regions with significant SH change, red box highlight decrease*
 210 *and blue-dashed box highlight increase.*

211

212 **3.2. Sensitivity of Spatial Homogeneity (Spatial Extent) to temperature.**

213 To comprehensively understand the effect of local climate and atmosphere on the spatial extent
 214 of extreme storms, a sensitivity analysis of spatial extent with temperature, intensity of
 215 precipitation and total column water vapor is performed. Sensitivity of spatial extent with
 216 instantaneous temperature is presented in Figure 3. A $1^{\circ}\times 1^{\circ}$ moving median is applied to smooth
 217 out the variability. ERA5-land provides hourly temperature data, but GPM provides 30-min
 218 precipitation so the instantaneous temperature here refers to the temperature at the time of the
 219 storm or in the hour before the storm. It is evident from the study that the tropical regions

220 dominated by convective precipitation have strong negative relation between spatial extent and
221 instantaneous temperature. This implies that as temperature rises, the convective storms in
222 tropics shrink in size and the moisture concentrates at the center. Parts of the Amazon and
223 Indonesian Tropical Regions observe 4-5%/°C reduction in spatial extent. On the other hand, the
224 arid regions particularly Eastern Sahara, the Thar desert in India, Southern Arabian Peninsula,
225 Gobi Desert and Western Coast of United States show positive sensitivity and will observe
226 spatially larger storms with the warming climate. The northern and southern temperate regions
227 generally present slight positive sensitivity of spatial extent with temperature with slightly
228 negative sensitivity seen in central and northern Europe (0.1-1%/°C), southern New Zealand and
229 Southern Argentina (Patagonian Dessert) (0.1-1.5%/°C).

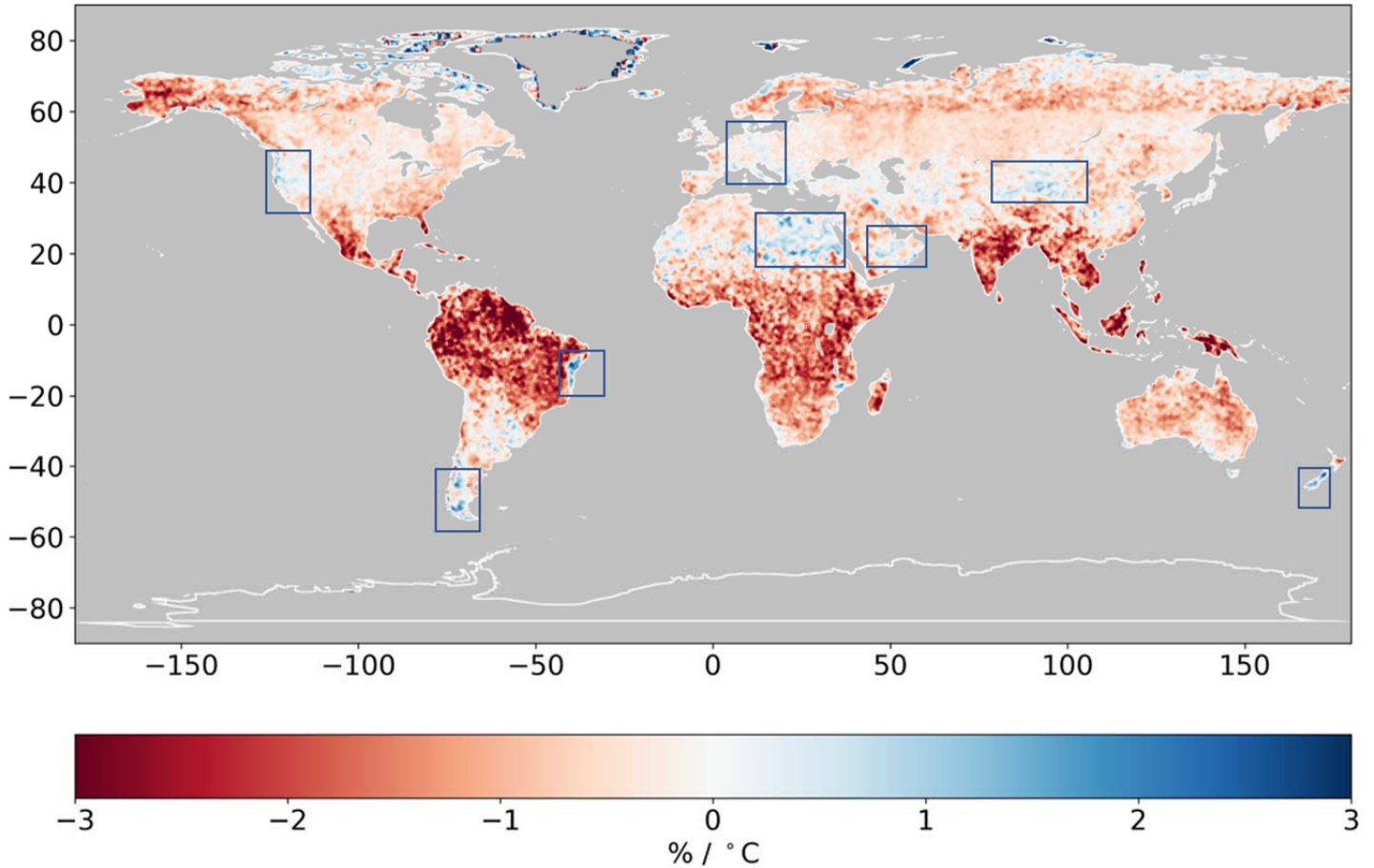
230

231 This study uses instantaneous temperature rather than widely used mean daily temperature
232 (Lenderink & van Meijgaard, 2008) because in case of convective storms, particularly in the
233 tropics, temperature tends to drop at the advent of the storm and using daily temperature for
234 sensitivity will result in inaccurate conclusions (Ali et al., 2018; Ali & Mishra, 2017). On
235 comparing the results of Figure S3 and Figure 3, it is evident that the impact of using daily
236 versus instantaneous temperature is concentrated in the equatorial regions. (Figure S3 in
237 supporting information presents the sensitivity of spatial extent with mean daily temperature).
238 Moreover, the sensitivity of spatial extent with instantaneous temperature is consistent and is
239 conformable to the recommendations by (Visser et al., 2020).

240

241 The results from this study are coherent with the findings from both Wasko et al. (2016) and
242 Lochbihler et al. (2017) which published contrasting results. While Wasko et al. (2016)
243 concluded a reduction in spatial extents in Australia, Lochbihler et al. (2017) concluded an
244 increase in spatial extent in Netherlands. This study finds that both the findings are accurate and
245 the behavior of spatial extent with temperature is indeed dependent on the geographic location
246 and the local climate.

247



248 *Figure 3. $1^{\circ}\times 1^{\circ}$ median of 50th percentile quantile regression of SH with instantaneous*
 249 *temperature. Negative sensitivity (decrease in SH with rising temperatures) is shown in red and*
 250 *Positive sensitivity (increase in SH with rising temperature) is shown in blue. Blue boxes*
 251 *highlight regions with negative sensitivity.*

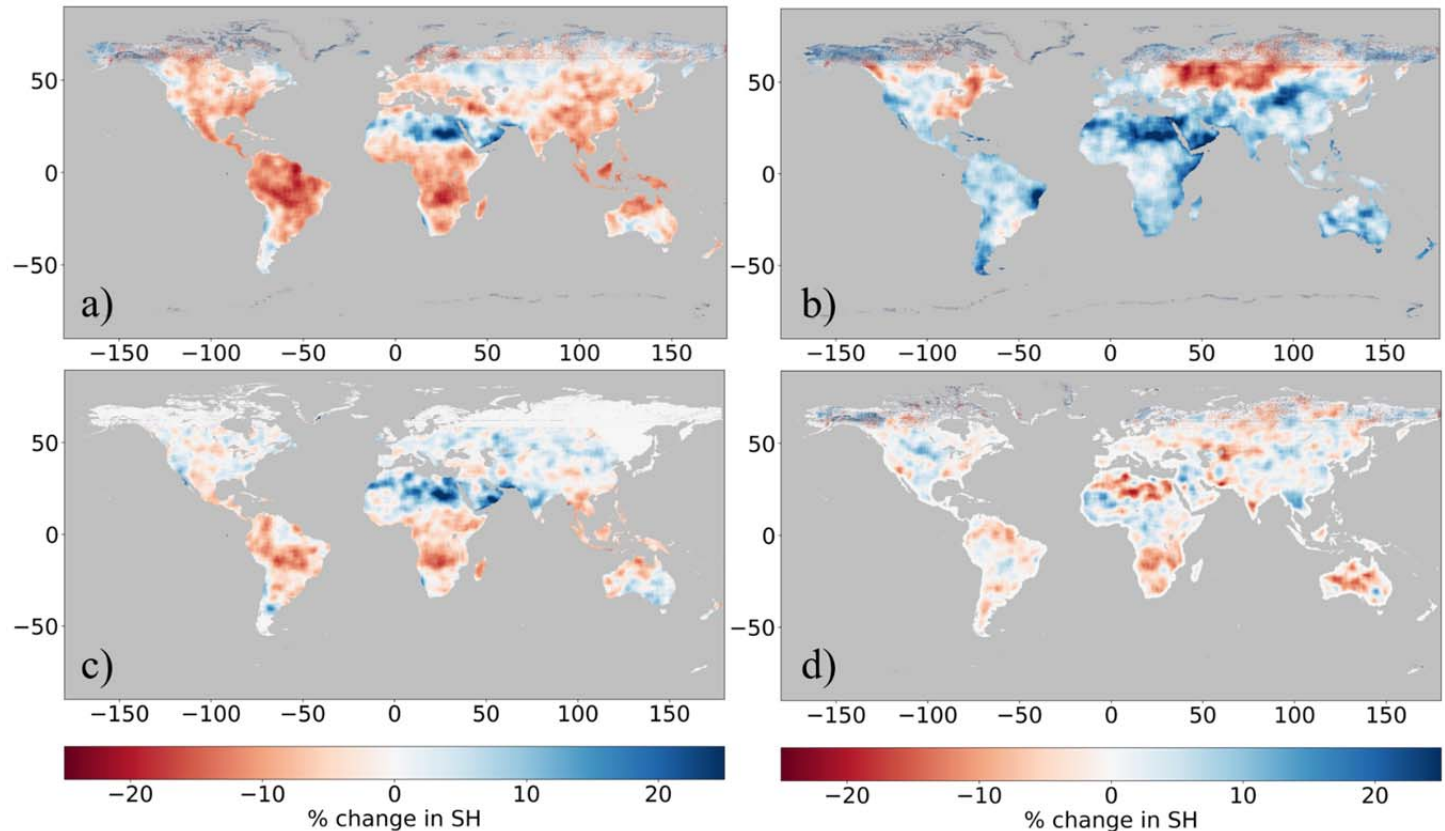
252

253 **3.3. Effect of local climate on Spatial Homogeneity (Spatial Extent).**

254 To assess the impact of local climate on SH, variation of the difference in SH associated with:
 255 maximum and minimum intensity storm (Figure 4a), maximum total column water vapor and
 256 minimum total column water vapor (Figure 4b), wettest and driest year storm (Figure 4c), and
 257 warmest and coldest year storm (Figure 4d) is mapped. At any location, the annual maxima
 258 storm with maximum precipitation intensity / maximum accumulated total column water vapor
 259 in 24hr prior to the storm is compared to the annual storm with minimum precipitation intensity /
 260 minimum accumulated total column water vapor in 24hr prior to the storm. Among the 2014-
 261 2021 period, the wettest and driest years at any location are estimated by comparing the total

262 annual precipitation, and warmest and coldest year are estimated by comparing the mean annual
 263 temperature.

264



265 *Figure 4. Change in SH when comparing SH corresponding to (a) Maximum vs Minimum*
 266 *Intensity storms, (b) Maximum vs Minimum Total Column Water Vapor Storms, (c) Wettest vs*
 267 *Driest Year storms and (d) Warmest vs Coldest Storms. Red indicates decrease in SH and blue*
 268 *indicates increase in SH*

269 The overall trend indicates that globally a rise in intensity of storms leads to a lower spatial
 270 extent (Figure 4a). A larger spatial extent for more intense storms is observed in Sahara, Arabian
 271 Peninsula, Central Russia, and southern Argentina (Patagonian Dessert). The overall global trend
 272 corroborates with the findings by Wasko et al. (2016) for Australia (extended here to a global
 273 scale) that the moisture is being redistributed from storm boundaries to the storm center. The
 274 findings from Figure 4a and Figure 3 support the hypothesis presented in Figure 1a implying that
 275 a rise in temperature will result in more intense and spatially concentrated extreme storm bursts.
 276 Moreover, the findings by Lochbihler et al. (2017) are also corroborated in Arid Regions around

277 the world. On the other hand, total column water vapor (TCWV) has an overall reinforcing
278 relation with the SH. A rise in TCWV results in greater SH implying that at most locations, with
279 exceptions of Eastern US and around central Russia, spatially larger storms are associated with
280 higher TCWV (Figure 4b). The effect of total annual precipitation is regionally distinct as
281 Sahara, Arabian Peninsula, India, Central Asia and Europe have larger spatial extent storms in
282 wetter years. On the other hand, drier years observe larger spatial extent storms in tropical
283 regions in Southern America, Africa, South East Asia and Northern and Western Australia.
284 (Figure 4c). Mean annual temperature does not have a overall strong impact on SH globally and
285 difference in SH is evenly distributed with least variance among all the variables (Figure 4d).
286 The study here presents a preliminary analysis of the impact of local climate variables on change
287 in spatial extent and a more extensive analysis may result in significant regional trends.

288

289 **4. Discussion**

290

291 While the data length used in the study is shorter than that used for point-based studies of spatial
292 extent done in the past, it is interesting to note that the same conclusions are drawn from short
293 time period as the conclusions from longer duration time period (Figure S4 in supplementary
294 information provides sensitivity of SH with temperature for a time period of 2005-2021).

295

296 The study uses 9 grid cells (3x3 grid) to define the storm field and estimate SH. This 9-cell grid
297 structure implies that the storm field extends over 30x30 km which will be smaller than that
298 observed for daily storms, but it is sufficient for short duration (30 min) precipitation extremes. It
299 is noteworthy that using a larger size storm field (25 neighboring grid cells or more)
300 quantitatively changes the overall SH for short duration storms (Figure S5 (b)) however, using a
301 larger storm field does not alter the patterns for change in SH. The overall conclusions regarding
302 sensitivity of spatial extent (SH) with temperature and other parameters remain the same whether
303 using 9-cell storm field or 25-cell storm field (Figure S6).

304

305 These short duration storm systems are susceptible to presence of zero precipitation cells in the
306 storm field thus presenting larger inhomogeneity and less linearity in spatially accumulated
307 average precipitation. Although, the formulation of SH metric uses linear proportionality to

308 estimate the spatial homogeneity, a sensitivity analysis using non-linear proportionality to
309 calculate SH does not significantly alter SH estimates. This establishes that linear proportionality
310 can capture the spatial homogeneity even for short duration storms. It is also noteworthy that the
311 zero-precipitation cells primarily affect SH for precipitation sparse arid regions (Figure S5(a))
312 which are hotspots for increasing spatial extent with temperature.

313

314 **5. Conclusions**

315

316 There is clear understanding that intensity of extreme storms will increase with increase in
317 temperature but the studies on the spatial organization of storms have been conflicting. Use of
318 daily average temperatures instead of sub-daily temperatures, focus on specific regions, or on
319 certain type of storms, or at daily precipitation extremes rather than short duration storms;
320 contributed to conflicting results in previous studies. The results of this study show that the
321 geographic location and the local climate play a crucial role in how moisture is being distributed
322 around a storm, particularly for short duration extreme storms. The following conclusions are
323 drawn from this study:

- 324 1. Spatial extent of short duration precipitation extremes has increased in the equatorial
325 tropics and decreased in the northern and southern temperate in the recent past. However,
326 sensitivity of spatial extent with temperature has contrasting results.
- 327 2. An overall global trend of moisture accumulation towards the storm center as spatial
328 extent decreases with a rise in temperatures.
- 329 3. Spatial extent of storms in arid regions (excluding Australia) and parts of central Europe
330 tends to increase with increasing temperature.

331

332 Some other conclusions from the preliminary analysis with local climate variables can also be
333 made. Higher intensity storms typically result in lower spatial extent storms. Furthermore, the
334 study finds that spatially larger storms are globally associated with higher total precipitable
335 water. Wet years in Sahara, Arabian Peninsula, India, Central Asia and Europe have larger
336 spatial extent storms whereas dry years observe larger spatial extent storms in tropical regions in
337 Southern America, Africa, Southeast Asia, Northern and Western Australia. Warm vs Cold year

338 do not have a consistent impact on spatial extent, although a more regressive analysis will result
339 in concrete conclusions.

340

341 These results along with previous understanding that intensity of extreme storms increase in
342 warmer climate, have significant implications as short duration extreme storms in warmer
343 climate will be more intense and concentrated. If these trends of spatial extent continue as the
344 global temperature rise, the tropics may experience intense and concentrated storms which may
345 lead to severe floods.

346

347 Future studies may focus on analyzing if similar patterns on change in spatial extent (spatial
348 homogeneity) are observed for longer duration storms. This study concludes that short (sub-
349 hourly) extreme storms show significant change alteration in spatial extent, however the change
350 in spatial extent may not be equally conspicuous for longer duration storms. This is routed in the
351 fact that super CC scaling is observed for shorter (sub-hourly, hourly, sub-daily) duration storms
352 and becomes less prominent as the duration of storm increases.

353

354 **Data Availability Statement**

355

356 All observational datasets and model simulations used in this study are publicly available. ERA5
357 and ERA5-Land are available from the European Centre for Medium-Range Weather Forecasts'
358 (ECMWF) Copernicus Climate Change Service (C3S) Climate Data Store at
359 <https://cds.climate.copernicus.eu/cdsapp#!/dataset/reanalysis-era5-land?tab=overview> and
360 <https://cds.climate.copernicus.eu/cdsapp#!/dataset/reanalysis-era5-pressure-levels?tab=overview>.
361 GPM IMERG data are available at <https://gpm.nasa.gov/data>.

362

363 **References**

364 Adhikari, A., Liu, C., & Hayden, L. (2019). Uncertainties of GPM Microwave Imager
365 Precipitation Estimates Related to Precipitation System Size and Intensity. *Journal of*
366 *Hydrometeorology*, 20(9), 1907–1923. <https://doi.org/10.1175/JHM-D-19-0038.1>

- 367 Ali, H., Fowler, H. J., & Mishra, V. (2018). Global Observational Evidence of Strong Linkage
368 Between Dew Point Temperature and Precipitation Extremes. *Geophysical Research*
369 *Letters*, 45(22), 12, 312–320, 330. <https://doi.org/10.1029/2018GL080557>
- 370 Ali, H., & Mishra, V. (2017). Contrasting response of rainfall extremes to increase in surface air
371 and dewpoint temperatures at urban locations in India. *Scientific Reports*, 7(1), 1228.
372 <https://doi.org/10.1038/s41598-017-01306-1>
- 373 Archer, D. R., & Fowler, H. J. (2018). Characterising flash flood response to intense rainfall and
374 impacts using historical information and gauged data in Britain. *Journal of Flood Risk*
375 *Management*, 11(S1), S121–S133 <https://doi.org/10.1111/jfr3.12187>
- 376 Berg, P., Moseley, C., & Haerter, J. O. (2013). Strong increase in convective precipitation in
377 response to higher temperatures. *Nature Geoscience*, 6(3), 181–185.
378 <https://doi.org/10.1038/ngeo1731>
- 379 Bevacqua, E., Shepherd, T. G., Watson, P. A. G., Sparrow, S., Wallom, D., & Mitchell, D.
380 (2021). Larger Spatial Footprint of Wintertime Total Precipitation Extremes in a Warmer
381 Climate. *Geophysical Research Letters*, 48(8), e2020GL091990.
382 <https://doi.org/10.1029/2020GL091990>
- 383 Chang, W., Stein, M. L., Wang, J., Kotamarthi, V. R., & Moyer, E. J. (2016). Changes in
384 Spatiotemporal Precipitation Patterns in Changing Climate Conditions. *Journal of Climate*,
385 29(23), 8355–8376. <https://doi.org/10.1175/JCLI-D-15-0844.1>
- 386 Chen, Y., Paschalis, A., Kendon, E., Kim, D., & Onof, C. (2021). Changing Spatial Structure of
387 Summer Heavy Rainfall, Using Convection-Permitting Ensemble. *Geophysical Research*
388 *Letters*, 48(3), e2020GL090903. <https://doi.org/10.1029/2020GL090903>
- 389 Collins, M., Knutti, R., Arblaster, J., Dufresne, J., Fichet, T., Friedlingstein, P., Gao, X.,
390 Gutowski, W., Johns, T., Krinner, G., Shongwe, M., Tebaldi, C., Weaver, A., & Wehner, M.
391 (2013). Long-term Climate Change: Projections, Commitments and Irreversibility. In:
392 Climate Change 2013: The Physical Science. *Climate Change 2013 the Physical Science*
393 *Basis: Working Group I Contribution to the Fifth Assessment Report of the*
394 *Intergovernmental Panel on Climate Change, January 2014.*
- 395 Dinku, T., Connor, S. J., & Ceccato, P. (2010). Comparison of CMORPH and TRMM-3B42 over
396 mountainous regions of Africa and South America. *Satellite Rainfall Applications for*

- 397 *Surface Hydrology*, 193–204. [https://doi.org/10.1007/978-90-481-2915-](https://doi.org/10.1007/978-90-481-2915-7_11/FIGURES/11_5_164676_1_EN)
398 [7_11/FIGURES/11_5_164676_1_EN](https://doi.org/10.1007/978-90-481-2915-7_11/FIGURES/11_5_164676_1_EN)
- 399 Duan, Y., Wilson, A. M., & Barros, A. P. (2015). Scoping a field experiment: Error diagnostics
400 of TRMM precipitation radar estimates in complex terrain as a basis for IPHEX2014.
401 *Hydrology and Earth System Sciences*, 19(3), 1501–1520. [https://doi.org/10.5194/HESS-19-](https://doi.org/10.5194/HESS-19-1501-2015)
402 [1501-2015](https://doi.org/10.5194/HESS-19-1501-2015)
- 403 Guinard, K., Mailhot, A., & Caya, D. (2015). Projected changes in characteristics of precipitation
404 spatial structures over North America. *International Journal of Climatology*, 35(4), 596–
405 612. <https://doi.org/10.1002/joc.4006>
- 406 Han, X., Mehrotra, R., & Sharma, A. (2020). Measuring the spatial connectivity of extreme
407 rainfall. *Journal of Hydrology*, 590, 125510. <https://doi.org/10.1016/j.jhydrol.2020.125510>
- 408 Hapuarachchi, H. A. P., Wang, Q. J., & Pagano, T. C. (2011). A review of advances in flash
409 flood forecasting. *Hydrological Processes*, 25(18), 2771–2784.
410 <https://doi.org/10.1002/hyp.8040>
- 411 Hardwick Jones, R., Westra, S., & Sharma, A. (2010). Observed relationships between extreme
412 sub-daily precipitation, surface temperature, and relative humidity. *Geophysical Research*
413 *Letters*, 37(22). <https://doi.org/10.1029/2010GL045081>
- 414 Hersbach, H., Bell, B., Berrisford, P., Hirahara, S., Horányi, A., Muñoz-Sabater, J., Nicolas, J.,
415 Peubey, C., Radu, R., Schepers, D., Simmons, A., Soci, C., Abdalla, S., Abellan, X.,
416 Balsamo, G., Bechtold, P., Biavati, G., Bidlot, J., Bonavita, M., ... Thépaut, J.-N. (2020).
417 The ERA5 global reanalysis. *Q J R Meteorol Soc*, 146, 1999–2049.
418 <https://doi.org/10.1002/qj.3803>
- 419 Huffman, G. J., Bolvin, D. T., Braithwaite, D., Hsu, K.-L., Joyce, R. J., Kidd, C., Nelkin, E. J.,
420 Sorooshian, S., Stocker, E. F., Tan, J., Wolff, D. B., & Xie, P. (2020). Integrated Multi-
421 satellite Retrievals for the Global Precipitation Measurement (GPM) Mission (IMERG). In
422 V. Levizzani, C. Kidd, D. B. Kirschbaum, C. D. Kummerow, K. Nakamura, & F. J. Turk
423 (Eds.), *Satellite Precipitation Measurement: Volume 1* (pp. 343–353). Springer International
424 Publishing. https://doi.org/10.1007/978-3-030-24568-9_19
- 425 Kelsch Matthew and Caporali, E. and L. L. G. (2001). Hydrometeorology of Flash Floods. In J.
426 Grunfest Eve and Handmer (Ed.), *Coping With Flash Floods* (pp. 19–35). Springer
427 Netherlands. https://doi.org/10.1007/978-94-010-0918-8_4

- 428 Kharin, V. v, Zwiers, F. W., Zhang, X., & Wehner, M. (2013). Changes in temperature and
429 precipitation extremes in the CMIP5 ensemble. *Climatic Change*, *119*(2), 345–357.
430 <https://doi.org/10.1007/s10584-013-0705-8>
- 431 Kucera, P. A., & Klepp, C. (2022). Evaluation of high-resolution satellite precipitation over the
432 global oceans. *Precipitation Science*, 305–332. [https://doi.org/10.1016/B978-0-12-822973-](https://doi.org/10.1016/B978-0-12-822973-6.00008-1)
433 [6.00008-1](https://doi.org/10.1016/B978-0-12-822973-6.00008-1)
- 434 Lenderink, G., Barbero, R., Loriaux, J. M., & Fowler, H. J. (2017). Super-Clausius–Clapeyron
435 Scaling of Extreme Hourly Convective Precipitation and Its Relation to Large-Scale
436 Atmospheric Conditions. *Journal of Climate*, *30*(15), 6037–6052.
437 <https://doi.org/10.1175/JCLI-D-16-0808.1>
- 438 Lenderink, G., Mok, H. Y., Lee, T. C., & van Oldenborgh, G. J. (2011). Scaling and trends of
439 hourly precipitation extremes in two different climate zones – Hong Kong and the
440 Netherlands. *Hydrology and Earth System Sciences*, *15*(9), 3033–3041.
441 <https://doi.org/10.5194/hess-15-3033-2011>
- 442 Lenderink, G., & van Meijgaard, E. (2008). Increase in hourly precipitation extremes beyond
443 expectations from temperature changes. *Nature Geoscience*, *1*(8), 511–514.
444 <https://doi.org/10.1038/ngeo262>
- 445 Li, J., Wasko, C., Johnson, F., Evans, J. P., & Sharma, A. (2018). Can Regional Climate
446 Modeling Capture the Observed Changes in Spatial Organization of Extreme Storms at
447 Higher Temperatures? *Geophysical Research Letters*, *45*(9), 4475–4484.
448 <https://doi.org/10.1029/2018GL077716>
- 449 Li, R., Wang, K., & Qi, D. (2021). Event-Based Evaluation of the GPM Multisatellite Merged
450 Precipitation Product From 2014 to 2018 Over China: Methods and Results. *Journal of*
451 *Geophysical Research: Atmospheres*, *126*(1), e2020JD033692.
452 <https://doi.org/10.1029/2020JD033692>
- 453 Lochbihler, K., Lenderink, G., & Siebesma, A. P. (2017). The spatial extent of rainfall events
454 and its relation to precipitation scaling. *Geophysical Research Letters*, *44*(16), 8629–8636.
455 <https://doi.org/10.1002/2017GL074857>
- 456 Manola, I., van den Hurk, B., de Moel, H., & Aerts, J. C. J. H. (2018). Future extreme
457 precipitation intensities based on a historic event. *Hydrology and Earth System Sciences*,
458 *22*(7), 3777–3788. <https://doi.org/10.5194/hess-22-3777-2018>

- 459 Matte, D., Christensen, J. H., & Ozturk, T. (2022). Spatial extent of precipitation events: when
460 big is getting bigger. *Climate Dynamics*, 58(5), 1861–1875. [https://doi.org/10.1007/s00382-](https://doi.org/10.1007/s00382-021-05998-0)
461 021-05998-0
- 462 Mishra, V., Wallace, J. M., & Lettenmaier, D. P. (2012). Relationship between hourly extreme
463 precipitation and local air temperature in the United States. *Geophysical Research Letters*,
464 39(16). <https://doi.org/10.1029/2012GL052790>
- 465 Muñoz-Sabater, J., Dutra, E., Agust-Panareda, A., Albergel, C., Arduini, G., Balsamo, G.,
466 Boussetta, S., Choulga, M., Harrigan, S., Hersbach, H., Martens, B., Miralles, D. G., Piles,
467 M., Rodríguez-Fernández, N. J., Zsoter, E., Buontempo, C., & Thépaut, J.-N. (2021).
468 ERA5-Land: a state-of-the-art global reanalysis dataset for land applications. *Earth System*
469 *Science Data*, 13(9), 4349–4383. <https://doi.org/10.5194/essd-13-4349-2021>
- 470 Pall, P., Allen, M. R., & Stone, D. A. (2007). Testing the Clausius–Clapeyron constraint on
471 changes in extreme precipitation under CO2 warming. *Climate Dynamics*, 28(4), 351–363.
472 <https://doi.org/10.1007/s00382-006-0180-2>
- 473 Peleg, N., Marra, F., Fatichi, S., Molnar, P., Morin, E., Sharma, A., & Burlando, P. (2018).
474 Intensification of Convective Rain Cells at Warmer Temperatures Observed from High-
475 Resolution Weather Radar Data. *Journal of Hydrometeorology*, 19(4), 715–726.
476 <https://doi.org/10.1175/JHM-D-17-0158.1>
- 477 Roderick, T. P., Wasko, C., & Sharma, A. (2019). Atmospheric Moisture Measurements Explain
478 Increases in Tropical Rainfall Extremes. *Geophysical Research Letters*, 46(3), 1375–1382.
479 <https://doi.org/10.1029/2018GL080833>
- 480 Roderick, T. P., Wasko, C., & Sharma, A. (2020). An Improved Covariate for Projecting Future
481 Rainfall Extremes? *Water Resources Research*, 56(8), e2019WR026924.
482 <https://doi.org/10.1029/2019WR026924>
- 483 Sharma, A., Wasko, C., & Lettenmaier, D. P. (2018). If Precipitation Extremes Are Increasing,
484 Why Aren't Floods? *Water Resources Research*, 54(11), 8545–8551.
485 <https://doi.org/10.1029/2018WR023749>
- 486 Tan, X., Wu, X., & Liu, B. (2021). Global changes in the spatial extents of precipitation
487 extremes. *Environmental Research Letters*, 16(5), 54017. [https://doi.org/10.1088/1748-](https://doi.org/10.1088/1748-9326/abf462)
488 9326/abf462

- 489 Tebaldi, C., Hayhoe, K., Arblaster, J. M., & Meehl, G. A. (2006). Going to the Extremes.
490 *Climatic Change*, 79(3), 185–211. <https://doi.org/10.1007/s10584-006-9051-4>
- 491 Trenberth, K. E., Dai, A., Rasmussen, R. M., & Parsons, D. B. (2003). THE CHANGING
492 CHARACTER OF PRECIPITATION. *Bulletin of the American Meteorological Society*,
493 84(9), 1205–1217. <http://www.jstor.org/stable/26216879>
- 494 Utsumi, N., Seto, S., Kanae, S., Maeda, E. E., & Oki, T. (2011). Does higher surface temperature
495 intensify extreme precipitation? *Geophysical Research Letters*, 38(16).
496 <https://doi.org/10.1029/2011GL048426>
- 497 Visser, J. B., Wasko, C., Sharma, A., & Nathan, R. (2020). Resolving Inconsistencies in Extreme
498 Precipitation-Temperature Sensitivities. *Geophysical Research Letters*, 47(18),
499 e2020GL089723. <https://doi.org/10.1029/2020GL089723>
- 500 Visser, J. B., Wasko, C., Sharma, A., & Nathan, R. (2021). Eliminating the “Hook” in
501 Precipitation–Temperature Scaling. *Journal of Climate*, 34(23), 9535–9549.
502 <https://doi.org/10.1175/JCLI-D-21-0292.1>
- 503 Wasko, C., & Sharma, A. (2014). Quantile regression for investigating scaling of extreme
504 precipitation with temperature. *Water Resources Research*, 50(4), 3608–3614.
505 <https://doi.org/10.1002/2013WR015194>
- 506 Wasko, C., Sharma, A., & Westra, S. (2016). Reduced spatial extent of extreme storms at higher
507 temperatures. *Geophysical Research Letters*, 43(8), 4026–4032.
508 <https://doi.org/10.1002/2016GL068509>
- 509 Westra, S., Fowler, H. J., Evans, J. P., Alexander, L. v, Berg, P., Johnson, F., Kendon, E. J.,
510 Lenderink, G., & Roberts, N. M. (2014). Future changes to the intensity and frequency of
511 short-duration extreme rainfall. *Reviews of Geophysics*, 52(3), 522–555.
512 <https://doi.org/10.1002/2014RG000464>
- 513